ELECTRONIC PROPERTIES OF THIN FILM SILICON

R. Brüggemann, J.P. Kleider, C. Longeaud
Laboratoire de Génie Electrique de Paris (UMR 8507 CNRS), Supélec,
Universités Paris VI et XI, Plateau de Moulon, F-91192 Gif sur Yvette Cedex, France
Phone: (33)-1-69-85-16-45; Fax: (33)-1-69-41-83-18; Email: brueggemann@lgep.supelec.fr

ABSTRACT: We characterise thin-film silicon deposited on glass by different techniques namely solid-phase crystallisation of amorphous silicon, plasma-enhanced chemical vapour deposition and hot-wire chemical vapour deposition. Values of the mobility-lifetime products for both the majority and minority carriers of high-crystallinity material compare well with those of hydrogenated amorphous silicon-germanium alloys that are competitors for the application in photovoltaic devices. We relate these photoelectronic properties to subgap absorption and the density of states as derived from transient and modulated photoconductivity. As for microcrystalline silicon from plasma-enhanced chemical vapour deposition, we find no light-induced degradation for thin-film silicon samples from hot-wire chemical vapour deposition and from solid-phase crystallisation.

Keywords: Thin Film - 1: Si Films - 2: Photoelectric Properties - 3

1. INTRODUCTION

These proceedings and those of previous European Photovoltaic and Solar Energy Conferences document the interest that has developed in the application of thin film crystalline silicon in photovoltaic devices. Depending on the deposition method silicon can be prepared with a wide range in the value of crystallite grain size but little is known about the electronic properties of these heterogeneous materials and the relation of charge carriers to gap states that control transport and recombination.

We studied the electronic properties of thin film silicon on glass prepared by various deposition techniques. The films cover the range from amorphous silicon over nanocrystalline (nc) or so-called microcrystalline silicon (μc-Si) with nanometer-sized grains to polycrystalline silicon with grain sizes larger than 1000 Å. The latter films were prepared by solid-phase crystallisation (SPC) of amorphous silicon. Plasma-enhanced chemical vapour deposition (PECVD) and hot-wire chemical vapour deposition (HWCVD) were used for the microcrystalline and amorphous silicon samples. We also present structural information to indicate the crystalline character of the films.

The undoped thin-film Si samples were characterised with respect to majority and minority carrier mobility-lifetime products from steady-state photoconductivity (SSPC) and photocarrier grating (SSPG) experiments. We relate these results to the profile of the sub-gap absorption coefficient detected with the constant photocurrent method (CPM). We applied transient photoconductivity (TPC) and modulated photoconductivity (MPC) as tools to determine the density of states (DOS) below the conduction band edge (E_c). Finally, we also address the aspect of light-induced degradation in the thin-film crystalline Si samples.

2. EXPERIMENTAL

We characterised nominally undoped thin-film Si samples deposited on glass substrates at several laboratories and with different deposition techniques for which the references provide further details. We present results here on HWCVD μc-Si samples from Ecole Polytechnique, that were deposited in a high-vacuum deposition chamber [1] with a ratio *R*, defined as the silane to hydrogen flux $R = [SiH_4]/[H_2]$, of 5 and 7 %. Hot-wire μc-Si samples were also deposited at Institut für Physikalische Elektronik (*ipe*), Universität Stuttgart, in a high-vacuum and in an ultra-high-vacuum deposition system [2-5]. PECVD samples were deposited at *ipe* at an excitation frequency of 66 MHz [6]. We studied SPC poly-Si samples crystallised at 600°C from Université de Rennes I [7] and *ipe* [8]. The amorphous silicon films for the crystallisation stem from low pressure chemical vapour deposition (LPCVD) at 550 °C or PECVD at high substrate temperatures.

The samples were fitted with coplanar Al electrodes, 0.5 to 1 cm wide with gaps between 0.5 and 2 mm. Figure 1 shows that the current-voltage characteristics is Ohmic in such a configuration that we applied for our experiments.

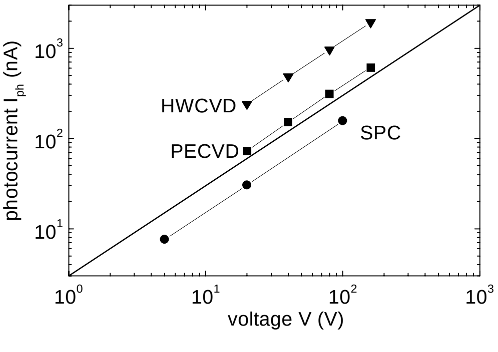

Figure 1: Current-voltage characteristics of HWCVD, PECVD and SPC Si samples show Ohmic behaviour. The diagonal represents current-voltage proportionality.

We applied an LED array or a HeNe laser for measuring photocurrents I_{ph} to calculate the photoconductivity σ_{ph} and mobility-lifetime product $\mu\tau$ representative of the majority-carrier properties. The ambipolar diffusion length L_d characteristic for the minority carriers was determined by the SSPG technique [9]. CPM [10] together with optical transmission and reflection provided details about optical absorption in the thin films. Details of the MPC experiment which measures the phase and amplitude of the photocurrent under intensity-modulated photogeneration can be found in Ref. 11. In the TPC experiment we studied the time-dependent photocurrent response after photoexcitation with a short laser pulse. The transient photocurrents are then converted into the DOS after Fourier transformation and use of appropriate equations [12].

Samples were light-soaked under water-filtered strong „white“ light illumination (500 mW/cm^2) for more than one day, both at 25°C and at 80°C. These measurements were performed under atmospheric pressure.

3. RESULTS

3.1 Structure

Figure 2 shows the Raman spectra for PECVD and HWCVD µc-Si films in comparison with results for SPC poly-Si and hydrogenated amorphous silicon. With caution, Raman spectroscopy serves as a tool to identify the crystalline volume fraction. The crystalline volume fraction R_C results from fitting the spectra and taking the ratio R_C of the areas under the fit curves of the amorphous (a) contribution and the crystalline (x) contributions according to $R_C = x/(x+a)$. The contribution from grain boundaries is included in the value for x.

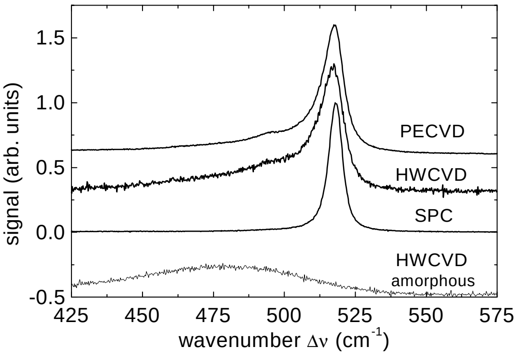

Figure 2: Raman spectra for an amorphous silicon HWCVD sample (bottom curve) and three thin-film crystalline samples with high crystallinity.

The SPC sample shows the typical Lorentzian shape as found for monocrystalline Si (c-Si) with no amorphous contribution, which peaks at much lower wavenumbers. The values of R_c of the PECVD and HWCVD µc-Si samples is between 70 and 80 %. These values can be taken as a lower limit of the crystalline volume fraction as R_c overestimates amorphous contributions to the Raman signal [13]. Lower values for R_c are possible [3] but the selection of samples in Figure 1 indicates that with adjustment of deposition parameters both PECVD and HWCVD techniques allow the deposition of films with high crystallinity.

3.2 Dark and steady-state photoconductive properties

Concerning the majority carrier properties Fig. 3 (a) summarises the dark conductivity σ_d values and $\mu\tau$ products for PECVD, HWCVD and SPC samples, at a photon flux ϕ of 10^{15} cm^{-2} s^{-1}. The labels for the different samples will be used throughout the text. Usually we find a relation between I_{ph} and ϕ given by $I_{ph} \propto \phi^{\gamma}$ with γ between 0.5 and 0.7. This means, as $\mu\tau \propto \phi^{\gamma-1}$, that values for $\mu\tau$ decrease for higher flux as compared to the data in Fig. 3.

The minority carrier properties are displayed in Fig. 3 (b) in terms of L_d, with the same abscissa scale. The L_d values of the PECVD and also of HWCVD µc-Si can be larger than 150 nm. Other HWCVD samples show quite low values of around 30 nm. SPC2 samples shows L_d larger than 500 nm.

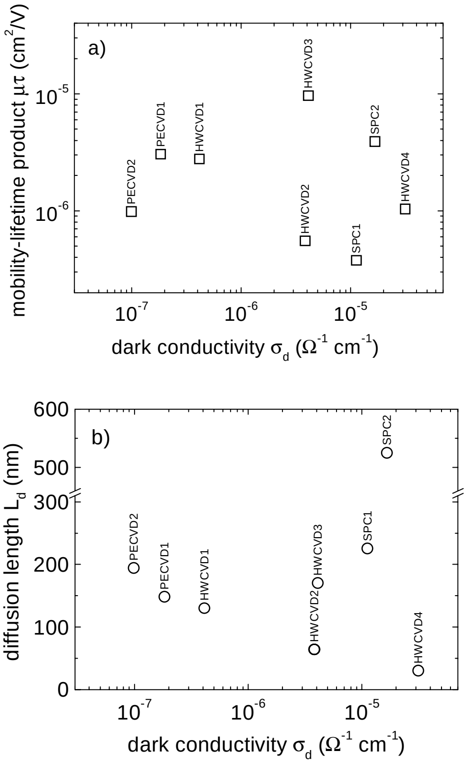

Figure 3: Mobility-lifetime products (a) and ambipolar diffusion lengths (b) vs. dark conductivity for a number of PECVD, HWCVD and SPC Si samples indicate the range of sample properties.

3.3 Subgap absorption

Figure 4 compares the absorption coefficient α of three µc-Si samples and one SPC sample. We plot here the measured and calibrated CPM signal together with α determined from optical spectroscopy at high energies.

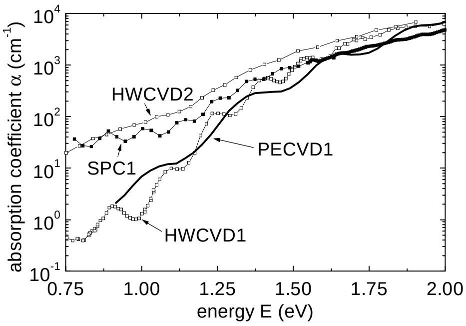

Figure 4: CPM-derived absorption spectra for HWCVD (open symbols) with low and high subgap absorption, PECVD (line) and SPC (full symbols) samples.

3.4 Density of states from modulated and transient photoconductivity

Figure 5 shows the TPC-derived DOS for three HWCVD samples, deposited at *R*= 5% (HWCVD3), *R* = 7% (HWCVD1), and *R*= 11%. The typical defect shoulder present in the amorphous film (*R*= 11%) [14] is not present in the µc-Si DOS that exhibits exponential energy dependence.

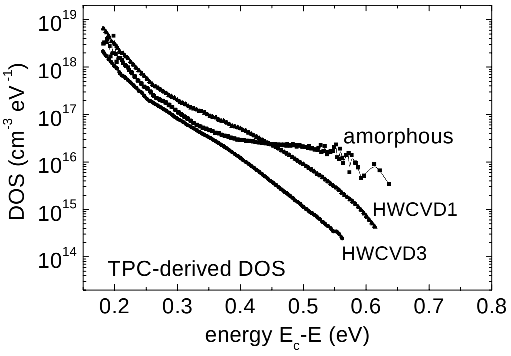

Figure 5: TPC-derived DOS for 3 HWCVD samples for different *R* values. The amorphous film at *R* = 11% shows a defect shoulder that disappears for the µc-Si sample at *R* = 5%.

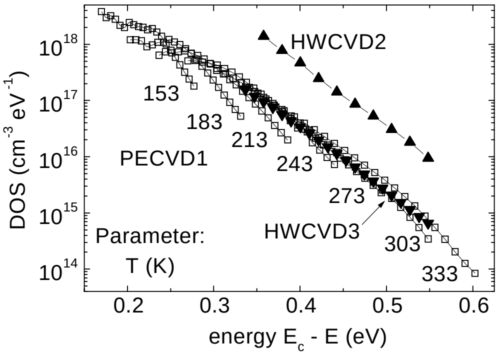

Figure 6: The set of MPC-derived DOS for PECVD1 sample (open symbols), taken at different *T,* exhibits an exponential increase towards the conduction band edge. The DOS of two HWCVD samples (full symbols) also shows the same trend.

The exponential shape of the DOS is also revealed in MPC-derived data. Indeed, Figure 6 shows a set of MPC data of the PECVD1 sample, taken at different temperatures *T* for which the overlap shows an exponential increase towards the conduction band edge E_c. Additional data are shown for HWCVD2 and HWCVD3 samples, that also exhibit the exponential shape of the DOS.

An exponentially increasing DOS towards E_c was also found for SPC poly-Si samples as displayed in Fig. 7. The energy variation in the set of MPC-derived DOS data is in good agreement with the TPC-derived DOS.

3.5 Light-induced degradation

Figure 8 shows the photocurrent under the conditions of light-soaking of the HWCVD1 sample that exhibits no decrease after more than 40 hours of light soaking. In addition, the displayed data for L_d measured before and after light-soaking, also show no decrease.

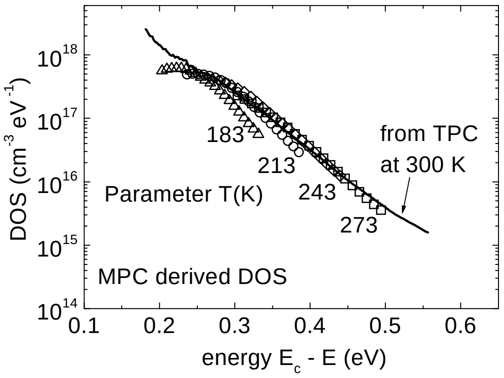

Figure 7: The set of MPC-derived DOS for an SPC sample, taken at different *T* exhibits exponential increase over a wide energy range in agreement with the TPC-derived DOS (line).

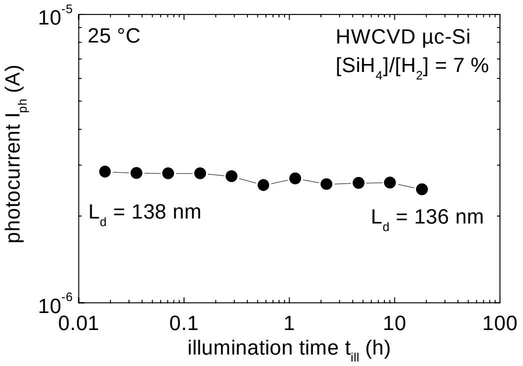

Figure 8: Light-soaking under intense illumination (500 mW/cm^2) does neither lead to a deterioration of the photocurrent, representing the majority carriers, nor affect the value for minority carrier property L_d.

4. DISCUSSION

We find a good correlation between transport properties, subgap absorption coefficient and densities of states. Indeed, comparing Figs. 3 and 4, we observe that HWCVD2 sample with the *high* subgap absorption shows the *lower* values for µτ and L_d. while HWCVD1 with the *low* subgap absorption is comparable with the PECVD1 sample, not only from the absorption values but also as far as the *high* µτ and L_d values are concerned. For the SPC samples, we also found that SPC2 which has the better transport properties has a lower subgap absorption (not shown in Fig. 4 for the sake of clarity). Note that the subgap absorption of our samples compares well with that of HWCVD µc-Si samples found in the literature [15] that show a pronounced shoulder in subgap absorption below 1.1 eV. Earlier results indicate higher values for subgap absorption in HWCVD as compared to PECVD µc-Si [4,6]. Here, the best HWCVD sample shows low subgap absorption comparable to PECVD samples.

It should be pointed out that this correlation between transport properties and subgap absorption is not a general rule, but is also dependent on the Fermi-level position and to some degree on optical scattering. The Fermi level can be changed either by intentional doping, surface effects or by non-intentional doping which may be caused by the adsorption of oxygen-containing species for instance. For highly conductive samples the Fermi-level position results in an increase in the electron lifetime by the filling of recombination centres with electrons, so that they may exhibit both a high μτ product and a high subgap absorption, as with HWCVD2 and HWCVD4. However, in that case, as Fig. 3 shows, the transport properties of holes are very poor, with a very low L_d.

Optical scattering may also influence the CPM-derived absorption spectra [5,16,17]. However, we find that the subgap absorption is still a good indicator for the photoelectronic properties in thinner samples where optical scattering is weak.

Comparing the transport properties (Fig. 3) and the DOS derived either from MPC or TPC (Figs. 5-6), we observe that a larger DOS is related to a lower μτ.

Finally, the results obtained on μc-Si samples compare well with that of a-SiGe:H thin films with band gap energies around 1.4 eV, that are competitors in PV applications. Indeed, values of the μτ products are generally below 10^{-6} cm^2 V^{-1} for these kinds of films [18]. Some samples exhibit higher values in the as-deposited or annealed state, but these fall again below 10^{-6} cm^2 V^{-1} after light-soaking [19]. On the contrary, no light degradation is found on the μc-Si thin films. This was already documented in the literature for PECVD samples [20], and we confirm it here for a HWCVD sample, with R= 7%. It is worth pointing out that no degradation was also observed for lower R values, with light-soaking being performed at either 25°C or 80°C.

We find a pronounced shoulder in the subgap absorption coefficient for the SPC samples but which have quite large values for μτ and L_d. As both mobility and lifetime determine the latter properties and by relating the shoulder to a relatively large density of recombination centres, determining τ, we suggest that the free carrier mobility in the poly-Si SPC samples is larger as compared to the μc-Si films for both electrons and holes.

5. CONCLUSION

The mobility-lifetime products and diffusion lengths of microcrystalline silicon from PECVD and HWCVD are in the range of those of hydrogenated amorphous silicon. The diffusion length of SPC poly-Si can be much larger than that of μc-Si. Both MPC and TPC determine exponentially distributed densities of states in the HWCVD and PECVD microcrystalline silicon and in the SPC polycrystalline silicon over a wide energy range. Any defect shoulder below the conducting band, prominent in hydrogenated amorphous silicon, is absent. Subgap absorption may serve as an indicator for the photoelectronic properties. While PECVD and SPC samples do not degrade upon light-soaking we also find no light-induced degradation in HWCVD μc-Si study for neither the majority nor the minority carrier properties.

ACKNOWLEDGEMENTS

R. B. acknowledges the Ministère des Affaires Etrangères, Paris, for support and the hospitality at *ipe* when performing CPM experiments there. This work was also supported by CNRS and ADEME within the ECODEV program. The authors thank C. Köhler for Raman measurements, and K. Brühne, H. Brummack, C. Zaczek, *ipe*, J. Guillet, J.E. Bourée, Ecole Polytechnique, T. Mohammed-Brahim, M. Sarret, Université de Rennes I, for samples preparation.

REFERENCES

[1] A. R. Middya, A. Lloret, J. Perrin, J. Huc, J. L. Moncel, J.Y. Parey, G. Rose, Mat. Res. Soc. Symposium Proceedings **377** (1995) 119.

[2] H.N. Wanka, M.B. Schubert, A. Hierzenberger, and V. Baumung, in Proceedings 14th European Photovoltaic Solar Energy Conference, Barcelona, 1997, edited by H.A. Ossenbrink et al. (Stephens & Associates, Bedford, U.K., 1997), p. 1005.

[3] R. Brüggemann, J.P. Kleider, C. Longeaud, D. Mencaraglia, J. Guillet, J.E. Bourée, C. Niikura, J. Non-Crystal. Solids **266-269** (2000) 258.

[4] R. Brüggemann, A. Hierzenberger, H.N. Wanka, M.B. Schubert, Mat. Res. Soc. Symposium Proceedings **507** (1999) 793.

[5] R. Brüggemann, A. Hierzenberger, P. Reinig, M. Rojahn, M. Schubert, S. Schweizer, H. Wanka, and I. Zrinscak, J. Non-Cryst. Solids **227-230** (1998) 982.

[6] H. Brummack, H.N. Wanka, A. Hierzenberger, R. Brüggemann, and M.B. Schubert, in Conf. Record 26th IEEE Photovoltaic Specialists Conference, Anaheim, 1997 (IEEE, New York, 1997), p. 679.

[7] R. Rogel, K. Kis-Sion, T. Mohammed-Brahim, O. Bonnaud, J.P. Kleider, in Proceedings 15th European Photovoltaic Solar Energy Conference, Vienna, 1998, edited by J. Schmid et al. (European Commission, Joint Research Centre, Ispra, 1998), p. 1701

[8] C. Zaczek, Thesis, *ipe*, 1998.

[9] D. Ritter, E. Zeldov, K. Weiser, Appl. Phys. Lett. **49** (1986) 791.

[10] M. Vanecek, J. Kocka, J. Stuchlik, A. Triska, Solid State Commun. **39** (1981) 1199.

[11] J. P. Kleider, C. Longeaud, Solid State Phenomena **44-46** (1995) 597.

[12] C. Main, R. Brüggemann, D.P. Webb, S. Reynolds, Solid State Comm. **83** (1992) 401.

[13] R. Carius, F. Finger, M. Luysberg, P. Hapke, and U. Backhausen, in Future Directions in Thin Film Science and Technology, edited by J.M. Marshall et al. (World Scientific, Singapore, 1996), p. 11.

[14] R. Brüggemann, C. Main, M. Rösch, D.P. Webb, , Mat. Res. Soc. Symp. Proceedings **420** (1996) 793.

[15] J.K. Rath, A. Barbon, and R.E.I. Schropp, J. Non-Cryst. Solids **227-230** (1998) 1277.

[16] A. Poruba, Z. Remes, J. Springer, M. Vanecek, A. Fejfar, J. Kocka, J. Meier, P. Torres, A. Shah, as Ref. 17, p. 781.

[17] R. Brüggemann, F. Houzé, these proceedings.

[18] W. Paul, J. H. Chen, E. Z. Liu, A. E. Wetsel, P. Wickboldt, J. Non-Cryst. Solids **164-166** (1993) 1.

[19] J. P. Kleider, C. Longeaud, P. Roca i Cabarrocas, P. St'ahel, P. Sladek, in Proceedings 15th European Photovoltaic Solar Energy Conference, Vienna, 1998, edited by J. Schmid et al. (European Commission, Joint Research Centre, Ispra, 1998), p. 838.

[20] M. Goerlitzer, N. Beck, P. Torres, U. Kroll, H. Keppner, J. Meier, J. Koehler, N. Wyrsch, A. Shah, Mat. Res. Soc. Symp. Proceedings **467** (1997) 301.